

Influences of tool pin profile and tool shoulder diameter on the formation of friction stir processing zone in AA6061 aluminium alloy

K. Elangovan, V. Balasubramanian *

Department of Manufacturing Engineering, Annamalai University, Annamalai Nagar 608 002, Tamil Nadu, India

Received 20 October 2006; accepted 29 January 2007

Available online 22 February 2007

Abstract

AA6061 aluminium alloy (Al–Mg–Si alloy) has gathered wide acceptance in the fabrication of light weight structures requiring a high strength-to-weight ratio and good corrosion resistance. Compared to the fusion welding processes that are routinely used for joining structural aluminium alloys, friction stir welding (FSW) process is an emerging solid state joining process in which the material that is being welded does not melt and recast. This process uses a non-consumable tool to generate frictional heat in the abutting surfaces. The welding parameters such as tool rotational speed, welding speed, axial force, etc., and tool pin profile play a major role in deciding the weld quality. In this investigation an attempt has been made to understand the effect of tool pin profile and tool shoulder diameter on FSP zone formation in AA6061 aluminium alloy. Five different tool pin profiles (straight cylindrical, tapered cylindrical, threaded cylindrical, triangular and square) with three different shoulder diameters have been used to fabricate the joints. The formation of FSP zone has been analysed macroscopically. Tensile properties of the joints have been evaluated and correlated with the FSP zone formation. From this investigation it is found that the square pin profiled tool with 18 mm shoulder diameter produced mechanically sound and metallurgically defect free welds compared to other tool pin profiles.

© 2007 Elsevier Ltd. All rights reserved.

Keywords: AA6061 aluminium alloy; Friction stir welding; Tool pin profile; Tool shoulder diameter; FSP zone; Tensile properties

1. Introduction

Heat treatable wrought aluminium–magnesium–silicon alloys conforming to AA6061 are of moderate strength and possess excellent welding characteristics over the high strength aluminium alloys. Hence, alloys of this class are extensively employed in marine frames, pipelines, storage tanks and aircraft applications. Although Al–Mg–Si alloys are readily weldable, they suffer from severe softening in the heat affected zone (HAZ) because of reversion (dissolu-

tion) of Mg₂Si precipitates during weld thermal cycle. This type of mechanical impairment presents a major problem in engineering design. It will be more appropriate to overcome or minimize the HAZ softening to improve mechanical properties of weldments [1].

Weld fusion zones typically exhibit coarse columnar grains because of the prevailing thermal conditions during weld metal solidification. This often results inferior weld mechanical properties and poor resistance to hot cracking. While it is thus highly desirable to control solidification structure in welds, such control is often very difficult because of the higher temperatures and higher thermal gradients in welds in relation to castings and the epitaxial nature of the growth process [2]. Nevertheless, several methods for refining weld fusion zones have been tried with partial

* Corresponding author. Tel.: +91 4144 239734 (O)/241147 (R); mobile: +91 9443412249; fax: +91 4144 239734 (O)/238275 (R).

E-mail addresses: elamko@rediffmail.com (K. Elangovan), visvabalu@yahoo.com (V. Balasubramanian).

success in the past: inoculation with heterogeneous nucleants, microcooler additions, surface nucleation induced by gas impingement and introduction of physical disturbance through techniques such as magnetic arc oscillation and pulsed current welding [3].

Compared to many of the fusion welding processes that are routinely used for joining structural alloys, friction stir welding (FSW) is an emerging solid state joining process in which the material that is being welded does not melt and recast. Friction stir welding (FSW) was invented at The Welding Institute (TWI), UK in 1991. Friction stir welding is a continuous, hot shear, autogenous process involving non-consumable rotating tool of harder material than the substrate material. Fig. 1 explains the working principle of FSW process. Defect free welds with good mechanical properties have been made in a variety of aluminium alloys, even those previously thought to be not weldable. When alloys are friction stir welded, phase transformations that occur during the cool down of the weld are of a solid state type. Due to the absence of parent metal melting, the new FSW process is observed to offer several advantages over fusion welding [4–6].

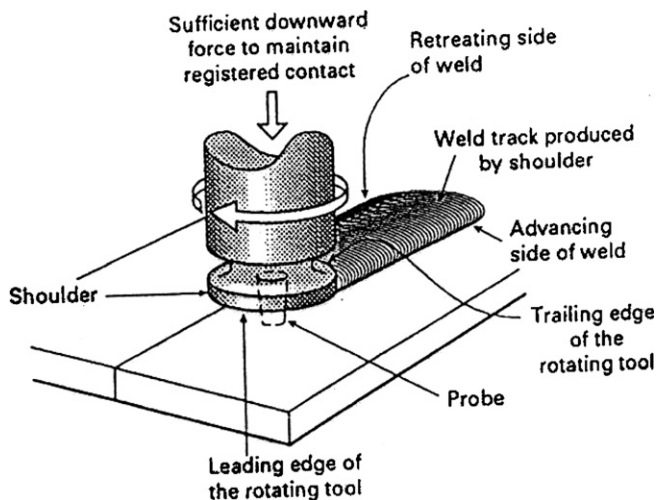
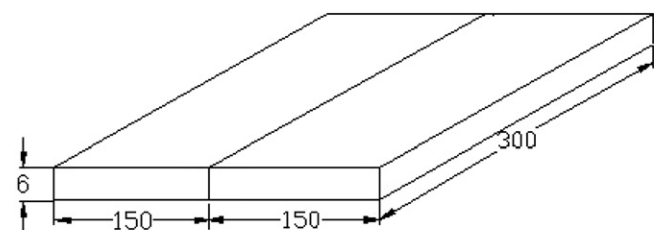


Fig. 1. Schematic representation of FSW principle.

FSW joints usually consist of four different regions as shown in Fig. 2. They are: (a) unaffected base metal, (b) heat affected zone (HAZ), (c) thermo-mechanically affected zone (TMAZ) and (d) friction stir processed (FSP) zone. The formation of above regions is affected by the material flow behaviour under the action of rotating non-consumable tool [7]. However, the material flow behaviour is predominantly influenced by the FSW tool profiles, FSW tool dimensions and FSW process parameters [8,9]. The available literature focusing on the effect of tool profiles and tool shoulder diameter on FSP zone formation is very minimal. Hence, in this investigation an attempt has been made to understand the effect of tool profiles and tool shoulder diameter on FSP zone formation. This paper presents the relation between the FSP zone formation and tensile properties of friction stir welded AA6061 aluminium alloy joints.

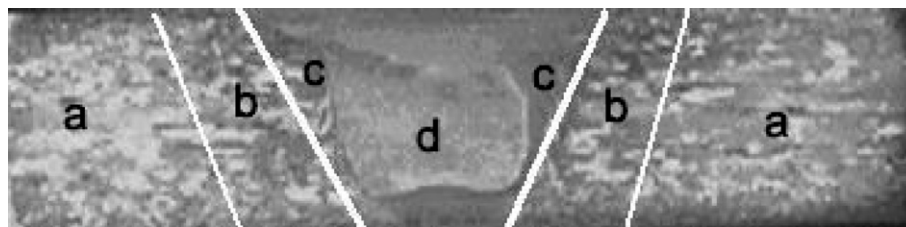
2. Experimental work

The rolled plates of 6 mm thickness, AA6061 aluminium alloy, have been cut into the required size (300 × 150 mm) by power hacksaw cutting and milling. Square butt joint configuration, as shown in Fig. 3 has been prepared to fabricate FSW joints. The initial joint configuration is obtained by securing the plates in position using mechanical clamps. The direction of welding is normal to the rolling direction. Single pass welding procedure has been followed to fabricate the joints. Non-consumable tools



(All the dimensions are in mm)

Fig. 3. Dimensions of square butt joint.



- a = Unaffected Base Metal
- b = Heat Affected Zone (HAZ)
- c = Thermo-Mechanically Affected Zone (TMAZ)
- d = Friction Stir Processed (FSP) Zone

Fig. 2. Different regions of FSW joint.

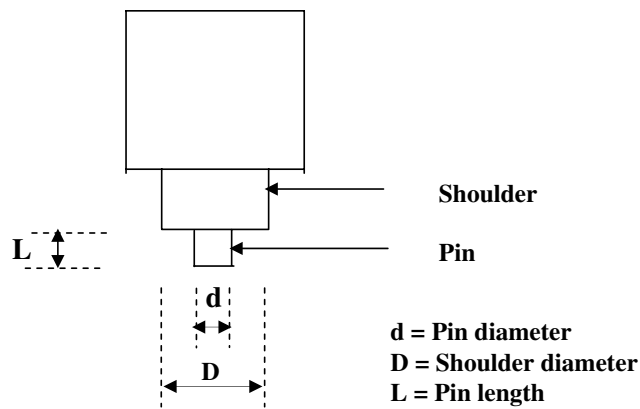


Fig. 4. FSW tool dimensions.

Table 1a
Chemical composition (wt%) of base metal

Elements	Mg	Mn	Fe	Si	Cu	Al
Base metal (6061-T ₆)	1.1	0.12	0.35	0.58	0.22	Bal

Table 1b
Mechanical properties of base metal

Material	Yield strength (MPa)	Ultimate tensile strength (MPa)	Elongation (%)	Vicker's hardness (0.5 kg)
Base metal	235	283	26.4	105

made of high carbon steel have been used to fabricate the joints. The tool dimensions are shown in Fig. 4. The chemical composition and mechanical properties of base metal are presented in Table 1. An indigenously designed and developed machine (15 HP; 3000 RPM; 25 KN) has been used to fabricate the joints. Five different tool pin profiles, as shown in Fig. 5 have been used to fabricate the joints. In each pin profile, three tools have been fabricated with three different shoulder diameters (*D*) and in total 15 tools (5 × 3)

have been fabricated. Each tool is used to fabricate one square butt joint and hence 15 joints have been fabricated in this investigation. The welding parameters and tool dimensions are presented in Table 2.

The welded joints are sliced using power hacksaw and then machined to the required dimensions to prepare tensile specimens as shown in Fig. 6. American Society for Testing of Materials (ASTM) guidelines are followed for preparing the test specimens. Tensile test has been carried out in 100 KN, electro-mechanical controlled Universal Testing Machine. The specimen is loaded at the rate of 1.5 KN/min as per ASTM specifications, so that tensile specimen undergoes deformation. The specimen finally fails after necking and the load versus displacement has been recorded. The 0.2% offset yield strength, ultimate tensile strength and percentage of elongation have been evaluated. Vicker's microhardness testing machine (make:

Table 2
Welding parameters and tool dimensions

Process parameters	Values
Rotational speed (RPM)	1200
Welding speed (mm/s)	1.25
Axial force (KN)	7.0
<i>D/d</i> ratio of tool	2.5, 3.0 and 3.5
Pin length (mm)	5.5
Tool shoulder diameter, <i>D</i> (mm)	15, 18 and 21
Pin diameter, <i>d</i> (mm)	6

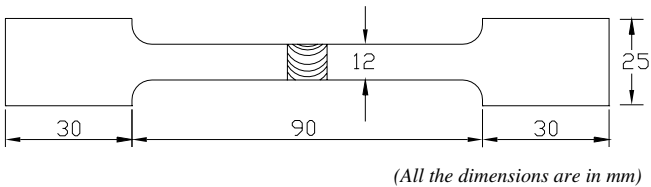


Fig. 6. Dimensions of tensile specimen.

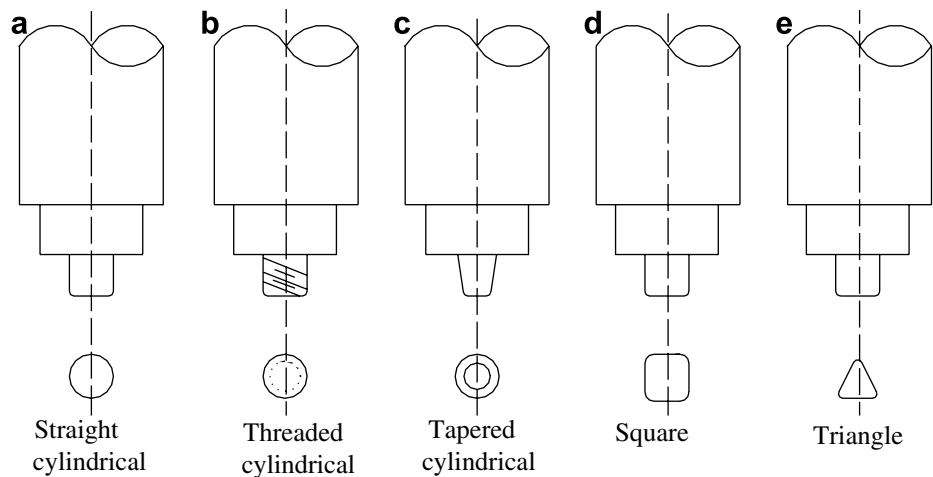


Fig. 5. FSW tool pin profiles.

Table 3
Macrostructure and observations of the joints fabricated by Straight Cylindrical (SC) pin profiled tool



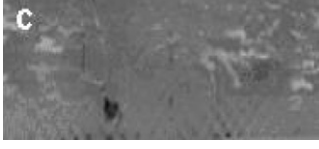


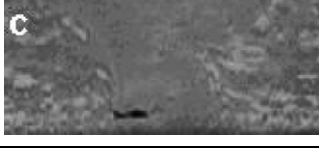
Shoulder diameter (mm)	Macrostructure		Size of FSP zone (mm)		Shape of FSP zone	Name of the defect and location	Quality of weld metal consolidation	Probable reason
	RS	AS	W	H				
15			10 6 5	5.9	Inverted trapezoidal	Tunnel in the bottom portion at the retreating side of the weld	Poor	Insufficient heat generation due to smaller shoulder contact area
18			8 6 4.6	5.9	Elliptical	No defect	Good	Sufficient heat generation and flow of the metal
21			10.8 6.1 5	5.9	Not discernible	Tunnel in the bottom portion at the retreating side of the weld	Poor	Excess heat generation and working of the metal

Table 4
Macrostructure and observations of the joints fabricated by Tapered Cylindrical (TC) pin profiled tool

Shoulder diameter (mm)	Macrostructure		Size of FSP zone (mm)		Shape of FSP zone	Name of the defect and location	Quality of weld metal consolidation	Probable reason
	RS	AS	W	H				
15			8.6 5 4.1	5.9	Inverted trapezoidal	Crack in the bottom portion of the weld at the retreating side	Poor	Insufficient heat generation due to smaller shoulder contact area
18			8.6 5 4.2	5.8	Inverted trapezoidal	No defect	Good	Sufficient heat generation and flow of the metal
21			8 5.3 4	5.9	Inverted trapezoidal	Tunnel in the bottom portion of the weld at the retreating side	Poor	Excess heat generation and flow of the metal in the weld zone

Matsumura, Japan; model: MMT-X7) has been employed for measuring the hardness across the joint with 0.5 kg load.

Macro and microstructural analysis have been carried out using a light optical microscope (make: Union Optical, Japan; model: VERSAMET-3) incorporated with an image analyzing software. The specimens for metallographic examination are sectioned to the required sizes

from the joint comprising FSP zone, TMAZ, HAZ and base metal regions and polished using different grades of emery papers. Final polishing has been done using the diamond compound (1 μm particle size) in the disc polishing machine. Specimens are etched with Kellers reagent to reveal the macro and microstructures. The fractured surface of the tensile tested specimens has been captured using digital scanner at low magnification to study the general

Table 5
Macrostructure and observations of the joints fabricated by Threaded Cylindrical (TH) pin profiled tool







Shoulder diameter (mm)	Macrostructure		Size of FSP zone (mm)		Shape of FSP zone	Name of the defect and location	Quality of weld metal consolidation	Probable reason
	RS	AS	W	H				
15			10	5.9	Inverted trapezoidal	Pin hole at lower portion of the weld cross section in retreating side	Poor	Insufficient heat input due to smaller shoulder diameter
			10	5.3	Elliptical	No defect	Good	Sufficient heat input
			10	5.8	Not discernible	No defect	Good	Wider FSP due to excess heat input caused by bigger shoulder diameter
			6					
			5					
			6.6					
			4.3					

Table 6
Macrostructure and observations of the joints fabricated by Square (SQ) pin profiled tool

Shoulder diameter (mm)	Macrostructure		Size of FSP zone (mm)		Shape of FSP zone	Name of the defect and location	Quality of weld metal consolidation	Probable reason
	RS	AS	W	H				
15			9.6	5.9	Inverted trapezoidal	Tunnel defect in the bottom portion of weld at retreating side of the weld	Poor	Insufficient heat input due to smaller shoulder diameter
			11.3	5.9	Inverted trapezoidal	No defect	Good	Sufficient heat input and flow of metal caused by square profiled pin
			11.0	5.9	Inverted trapezoidal	No defect	Good	Wider FSP due to excess heat input caused by bigger shoulder diameter
			5					
			4.6					
			5.6					
			4.6					
			6.6					
			5.0					

mode of fracture pattern to establish the relationship between FSP zone and the fracture.

3. Results




3.1. Macrostructure

It is generally known that the fusion welding of aluminum alloys is accompanied by the defects like porosity, slag

inclusion, solidification cracks, etc., and these defects deteriorate the weld quality and joint properties. However, friction stir welded joints are known to be free from these defects since there is no melting takes place during welding and the metals are joined in the solid state itself due to the heat generated by the friction and flow of metal by the stirring action. But FSW joints are prone to other defects like pin hole, tunnel defect, piping defect, kissing bond, cracks, etc. due to improper plastic flow and insufficient consolida-

Table 7

Macrostructure and observations of the joints fabricated by Triangular (TR) pin profiled tool

Shoulder diameter (mm)	Macrostructure		Size of FSP zone (mm)		Shape of FSP zone	Name of the defect and location	Quality of weld metal consolidation	Probable reason
	RS	AS	W	H				
15			9.6 6.3 5.0	5.9	Inverted trapezoidal	Tunnel in bottom portion of the weld	Poor	Insufficient heat input due to smaller shoulder diameter
18			8.6 5.3 4.6	5.9	Inverted trapezoidal	No defect	Good	Sufficient heat input and working of metal caused by triangular profiled pin
21			9.3 6.6 5.6	5.9	Inverted trapezoidal	No defect	Good	Wider FSP due to excess heat input caused by bigger shoulder diameter

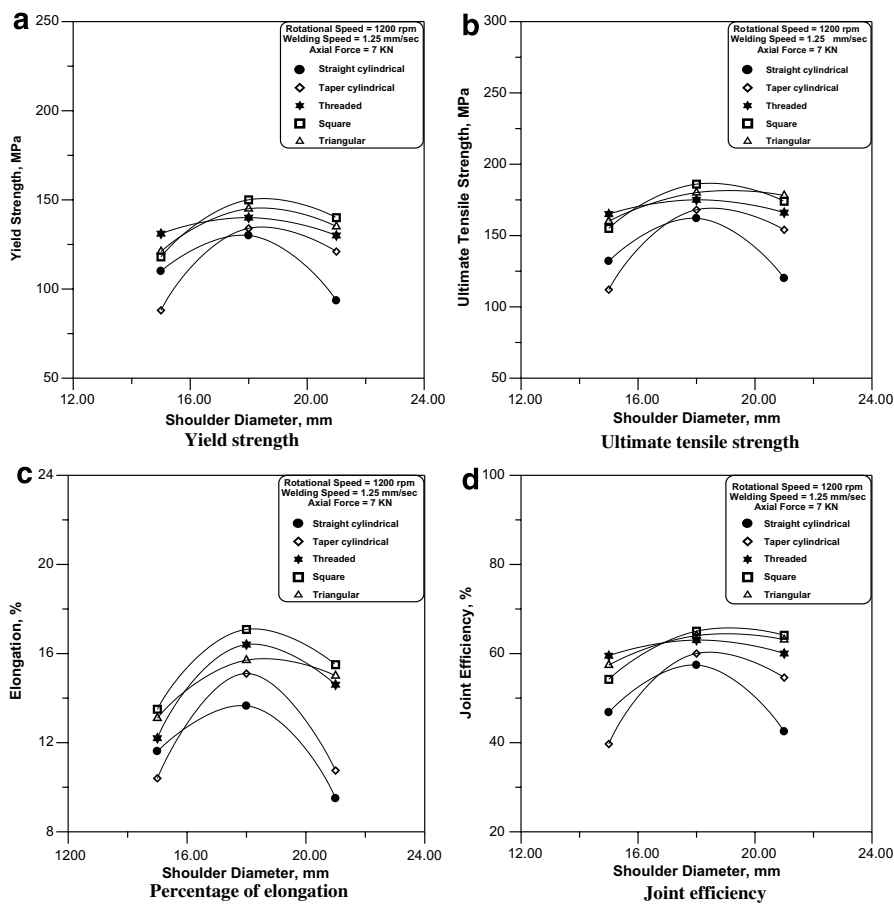


Fig. 7. Effect of tool shoulder diameter on tensile properties. (a) Yield strength, (b) ultimate tensile strength, (c) percentage of elongation, (d) joint efficiency.

Table 8
Fracture surface and observations of the joints fabricated by Straight Cylindrical (SC) pin profiled tool




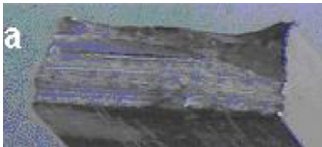
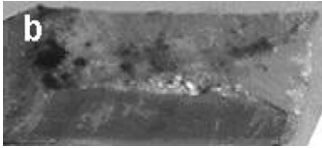

Shoulder diameter (mm)	Fracture surface	Location of fracture	Fracture surface appearance	Orientation of defects
15		Weld center along the joint line	Uneven surface with dull grey appearance and striations at the bottom	Groove at the bottom corresponding to the tunnel in the weld cross section
18		Between HAZ and FSP of the retreating side	Uneven surface with fibrous appearance and striations at the bottom	No defect
21		Between HAZ and FSP of the retreating side	Perfectly flat surface with bright granular appearance	Groove at the bottom corresponding to the tunnel in the weld cross section

Table 9
Fracture surface and observations of the joints fabricated by Tapered Cylindrical (TC) pin profiled tool

Shoulder diameter (mm)	Fracture surface	Location of fracture	Fracture surface appearance	Orientation of defects
15		Between HAZ and FSP of the retreating side	Flat surface with striations	Fine groove corresponding to the tunnel in the cross section
18		Between HAZ and FSP of the retreating side	Uneven fibrous surface with dull grey appearance	No defect
21		Between HAZ and FSP of the retreating side	Perfectly flat surface with bright granular appearance	Groove at the bottom corresponding to the tunnel in the weld cross section

tion of metal in the FSP region. All the joints fabricated in this investigation are analysed at low magnification (10×) using optical microscope to reveal the quality of FSP regions.

The macrostructure of the joints and the observations (FSP zone shape, FSP zone height (H), FSP zone width (W) at three different locations, quality of the FSP zone, etc.) made from the macrostructure are presented in Tables 3–7. Out of the three joints fabricated using straight cylindrical pin profiled tool (Table 3), the joint fabricated by a tool with shoulder diameter of 18 mm is found to be defect

free. Similarly, in the case of joints fabricated by tapered cylindrical pin profiled tool (Table 4), the joint fabricated by a tool with shoulder diameter of 18 mm is found to be defect free. In contrast, all the joints fabricated by threaded cylindrical pin profiled tool (Table 5), square pin profiled tool (Table 6) and triangular pin profiled tool (Table 7) are found to be free from all kind of defects except the joints fabricated by tools with shoulder diameter of 15 mm. From the macrostructure analysis, it can be inferred that the formation of defect free FSP zone is a function of tool profile and tool shoulder diameter.

Table 10

Fracture surface and observations of the joints fabricated by Threaded Cylindrical (TH) pin profiled tool




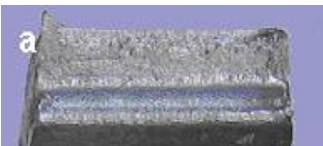


Shoulder diameter (mm)	Fracture surface	Location of fracture	Fracture surface appearance	Orientation of defects
15		In between HAZ and FSP at retreating side of the weld	Granular above and below the pin hole and striations in the groove	Groove along the weld axis corresponding to the pin hole in the weld cross section
18		In between HAZ and FSP at retreating side of the weld	Uneven surface with fibrous dull grey appearance	No defect
21		In between HAZ and FSP at retreating side of the weld	Concave surface with fibrous dull grey appearance	No defect

Table 11

Fracture surface and observations of the joints fabricated by Square (SQ) pin profiled tool

Shoulder diameter (mm)	Fracture surface	Location of fracture	Fracture surface appearance	Orientation of defects
15		In between HAZ and FSP at retreating side of the weld	Perfectly flat surface with bright granular appearance above the groove	Groove along the weld axis corresponding to the tunnel in the weld cross section
18		In between HAZ and FSP at retreating side of the weld	Uneven surface with fibrous dull grey appearance	No defect
21		In between HAZ and FSP at advancing side of the weld	Flat surface with granular appearance but tear ridges have observed at the edges	No defect




3.2. Tensile properties

Transverse tensile properties such as yield strength, tensile strength, percentage of elongation and joint efficiency of the FSW joints have been evaluated. At each condition three specimens are tested and average of the results of three specimens is presented in Fig. 7. From the figure, it can be inferred that the tool pin profile and tool shoulder diameter are having influence on tensile properties of the FSW joints. Of the five joints, the joints fabricated by square pin profiled

tool exhibited superior tensile properties compared to other joints, irrespective of tool shoulder diameter. Similarly, the joints fabricated by triangular pin profiled tool are also showing almost matching tensile properties to that of square pin. But the joints fabricated by straight cylindrical pin profiled tool exhibited inferior tensile properties compared to their counterparts, irrespective of tool shoulder diameter. The joints fabricated by the tools with shoulder diameter of 18 mm ($D/d = 3$) have shown higher tensile strength and elongation compared to the joints fabricated by the tools

Table 12

Fracture surface and observations of the joints fabricated by Triangular (TR) pin profiled tool

Shoulder diameter (mm)	Fracture surface	Location of fracture	Fracture surface appearance	Orientation of defects
15		Fracture along the weld joint line	Flat surface with bright granular appearance and striations at the root portion of the weld	Groove with striations along the weld axis corresponding to the tunnel in the weld cross section
18		In between FSP and HAZ at retreating side of the weld	Uneven surface with fibrous dull grey appearance	No defect
21		In between FSP and HAZ at retreating side of the weld	Flat surface with bright granular appearance	No defect

with shoulder diameter of 15 mm ($D/d = 2.5$) and this trend is common for all the tool pin profiles. Similarly, the joints fabricated by the tools with shoulder diameter of 21 mm ($D/d = 3.5$) have also shown lower tensile strength and elongation compared to the joints fabricated by the tools with shoulder diameter of 18 mm. The effect of shoulder diameter is concerned, the joints fabricated by the tools with shoulder diameter of 18 mm ($D/d = 3$) are showing superior tensile properties compared to other joints, irrespective of tool pin profiles. The fractured surface of the tensile test specimens was captured using a digital scanner and the fracture patterns of all the joints and the observations made from the fractured surface are presented in Tables 8–12. From the fractured surface analysis, it can be inferred that the defect free welds are showing uniform deformation across the weld before failure.

4. Discussion

From the experimental results (macrostructure, tensile properties and fracture surface), it is found that the joint fabricated using square pin profiled tool with the shoulder diameter of 18 mm exhibited superior tensile properties compared to other joints. The reasons for the better performance of these joints are explained below.

4.1. Effect of tool pin profile

The primary function of the non-consumable rotating tool pin is to stir the plasticized metal and move the same behind it to have good joint [10]. Pin profile plays a crucial role in material flow and in turn regulates the welding speed of the FSW process. The pin generally has cylindrical plain, frustum tapered, threaded and flat surfaces. Pin profiles with

flat faces (square and triangular) are associated with eccentricity. This eccentricity allows incompressible material to pass around the pin profile. Eccentricity of the rotating object is related to dynamic orbit due to eccentricity [11]. This dynamic orbit is the part of the FSW process. The relationship between the static volume and dynamic volume decides the path for the flow of plasticized material from the leading edge to the trailing edge of the rotating tool. This ratio is equal to 1 for straight cylindrical, 1.09 for tapered cylindrical, 1.01 for threaded cylindrical, 1.56 for square and 2.3 for triangular pin profiles. In addition, the triangular and square pin profiles produce a pulsating stirring action in the flowing material due to flat faces. The square pin profile produces 80 pulses/s and triangular pin profile produces 60 pulses/s when the tool rotates at a speed of 1200 rpm. There is no such pulsating action in the case of cylindrical, tapered and threaded pin profiles.

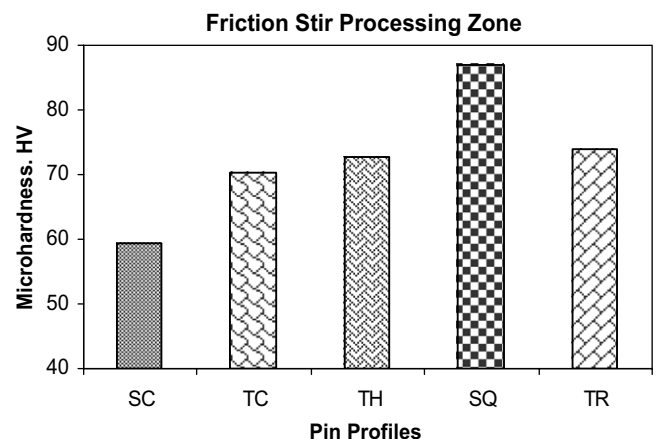


Fig. 8. Effect of pin profiles on FSP zone hardness.

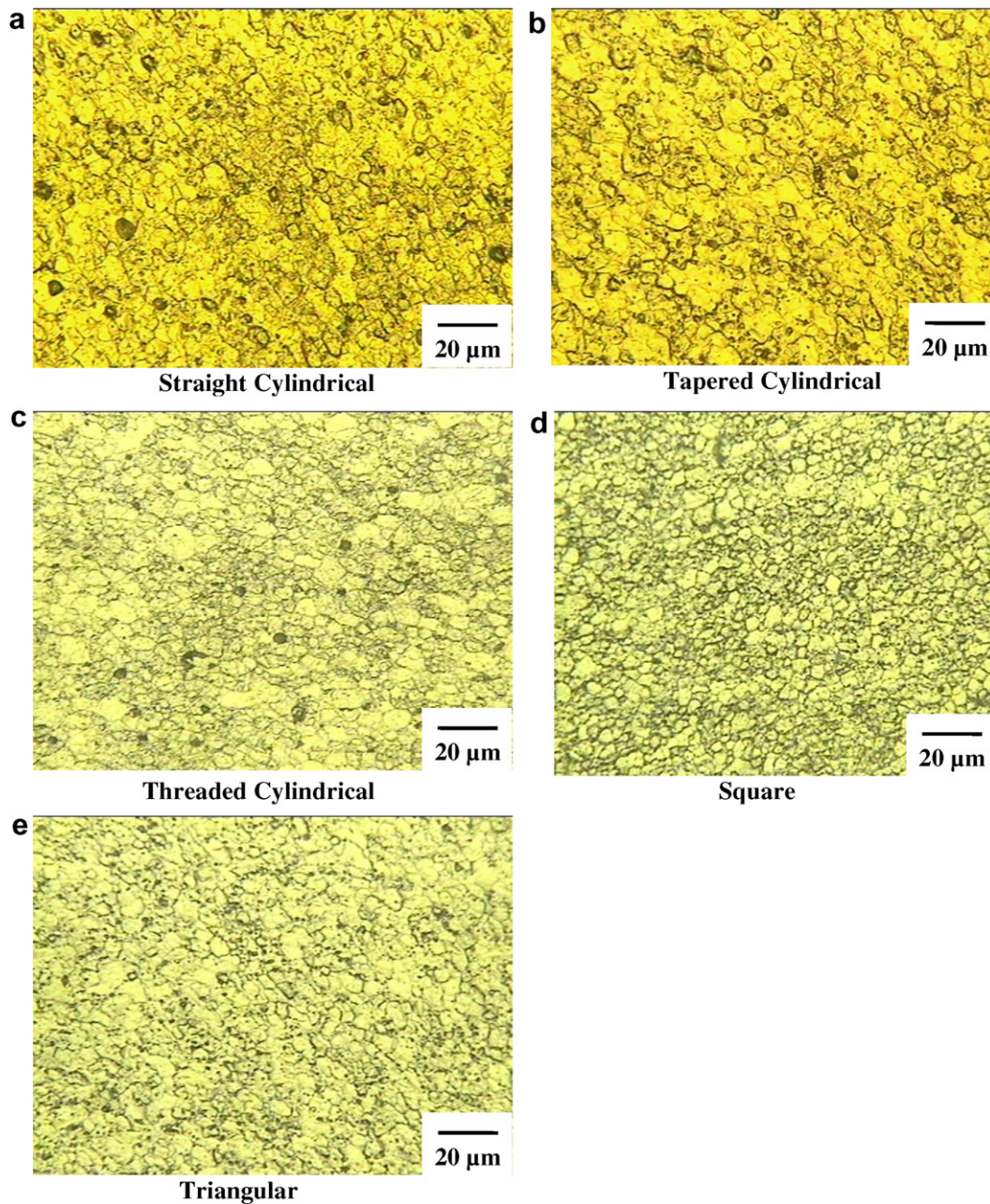


Fig. 9. Effect of tool profiles on microstructure of FSP zone. (a) Straight Cylindrical, (b) Tapered Cylindrical, (c) Threaded Cylindrical, (d) Square, (e) Triangular.

During tensile test, most of the specimens failed in the FSP region but the exact location of failure is either at the retreating side (RS) or at the advancing side (AS) and it is also evident from the fracture surface analysis. Hence, microhardness measurement and microstructural analysis have been carried out in the FSP region of all the joints. Fig. 8 shows the microhardness values and Fig. 9 displays the microstructure of FSP region of all the joints fabricated using the tools with 18 mm shoulder diameter for comparison purpose. Of the five joints, the highest hardness value of 88 VHN has been recorded in the joint fabricated using square pin profiled tool and the lowest hardness value of 60 VHN has been recorded in the joint fabricated using

straight cylindrical pin profiled tool. Similarly, the FSP region of the joint fabricated using square pin profiled tool contains very fine equiaxed microstructure (Fig. 9d) compared to other joints. The higher number of pulsating action experienced in the stir zone of square pin profile produces very fine microstructure and in turn yields higher strength and hardness.

4.2. Effect of tool shoulder diameter

Colligan [12] investigated the material flow behaviour of aluminium alloys during FSW and he opined that two effects are responsible for the creation of the material flow

in the FSP zone. First is the extrusion process, where the applied forces and the motion of the tool pin propel the material after it has undergone the plastic deformation. The second is due to the rotation of the pin that serves as the driving force for the flow. Due to high values of viscosity, the stirring effect is much more distinct in comparison to the extrusion driven flow. Ouyang et al. [13] visualized material flow behaviour during FSW of similar and dissimilar aluminium alloys and they found that in friction stir welds not all material influenced by the pin is actually “stirred” in the welding process. Much of the material movement takes place by simple extrusion. Modest vertical flow and material extrusion from front to back around both sides of the pin is possible and the role of the rotating pin is to provide frictional heating to make the extrusion possible.

Ying et al. [14] have studied the solid state flow visualization of FSW of AA2024 and AA6013 aluminium alloys and they observed that the flow of the plate material on the advancing side and the retreating side are different.

The material on the retreating side never enters into the rotational zone near the pin, but the material on the advancing side forms the fluidized bed near the pin and rotates around it. After several revolutions the material on the advancing side starts to slough off in the wake behind the pin. In the FSP zone the grain structure is characteristic of the idealized fluid particle concept which accommodates shear flow in liquid and liquid-like regimes. Lima et al. [15] and Oosterkamp et al. [16] have reported that at the top surface of the FSP region, a material transport occurs due to the action of the rotating tool shoulder. Material near the top of the FSP region, approximately the upper one-third, moves under the influence of the shoulder rather than the profiles on the pin.

The tool shoulder diameter is having directly proportional relationship with the heat generation due to friction [11]. If the shoulder diameter is large, then heat generation due to friction will be high due to large contact area and vice versa. In this investigation it has been observed that the larger tool shoulder diameter (21 mm) lead to wider contact area and resulted in wider TMAZ region and HAZ region and subsequently the tensile properties of the joints are deteriorated. It has been also observed that the smaller tool shoulder diameter (15 mm) lead to narrow contact area and resulted in less frictional heat generation and hence the weld metal consolidation is not good in the FSP region. Hence, the shoulder diameter must be optimized to get FSP region with good consolidation of metal and narrow region of TMAZ and HAZ regions.

Of the three different tool shoulder diameters used in this investigation, the joints fabricated using the tool with 18 mm shoulder diameter exhibited superior tensile properties, irrespective of tool pin profiles. For comparison purpose, the microhardness and microstructure of FSP zone produced by square pin profiled tool at different tool shoulder diameters are presented in Figs. 10 and 11. FSP zone hardness is higher in the joints fabricated using the tool with shoulder diameter of 18 mm compared to their counterparts. The joint fabricated using the tool with shoulder

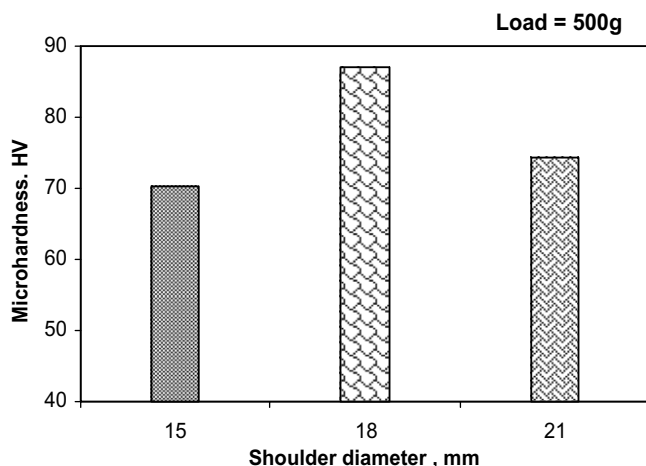


Fig. 10. Effect tool shoulder diameter on FSP zone hardness.

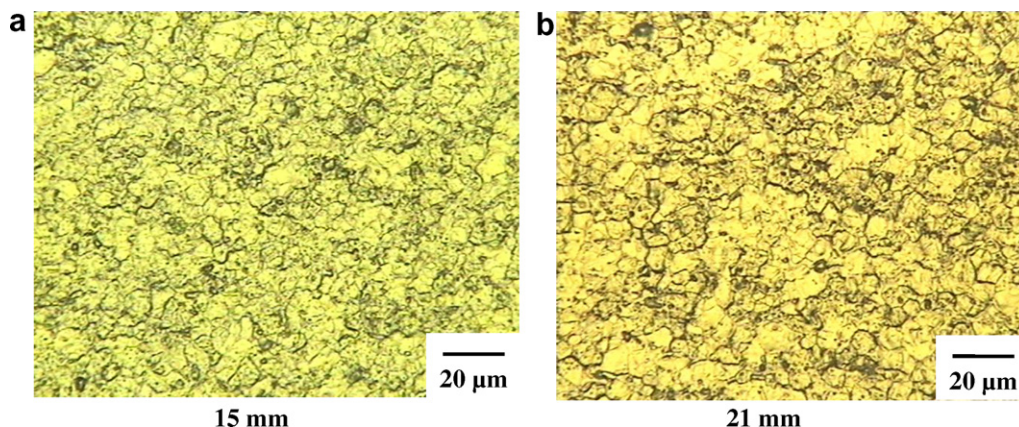


Fig. 11. Effect of tool shoulder diameter on microstructure of FSP zone (Tool profile: Square Pin).

diameter of 15 mm, consists of coarse grains (Fig. 11a) with bundle of strengthening precipitates (black particles). Similarly, the joint fabricated using the tool with shoulder diameter of 21 mm, consist of coarse grains (Fig. 11b) but the strengthening precipitates have become very fine and uniformly distributed throughout the matrix due to excessive axial force. But the joint fabricated using the tool with 18 mm diameter consist of fine, equiaxed grains with uniform distribution of fine strengthening precipitates throughout the matrix (Fig. 9d). This may be the reason for higher tensile strength and hardness of the joints fabricated using the tool with shoulder diameter of 18 mm compared to their counterparts. The combined effect of higher number of pulsating stirring action during metal flow and an optimum tool shoulder diameter may be the reason for superior tensile properties of the joint fabricated using square pin profiled tool with 18 mm shoulder diameter.

5. Conclusions

In this investigation an attempt has been made to study the effect of tool pin profile and tool shoulder diameter on the formation of friction stir processing zone in AA6061 aluminium alloy. From this investigation, the following important conclusions are derived:

- (i) Of the five tool pin profiles used in this investigation to fabricate the joints, square pin profiled tool produced defect free FSP region, irrespective of shoulder diameter of the tools.
- (ii) Of the three tool shoulder diameters used in this investigation to fabricate the joints, a tool with 18 mm shoulder diameter produced defect free FSP region, irrespective of tool pin profiles.
- (iii) Of the 15 joints fabricated in this investigation, the joint fabricated using square pin profiled tool with shoulder diameter of 18 mm showed superior tensile properties.

Acknowledgements

The authors are grateful to the Department of Manufacturing Engineering, Annamalai University, Annamalai Nagar, India for extending the facilities of Metal Joining Laboratory and Material Testing Laboratory to carryout this investigation. The authors wish to place their sincere

thanks to All India Council for Technical Education (AICTE), New Delhi for financial support rendered through a R&D project no. 8021/RID/NPROJ/R&D-89/2002-03.

References

- [1] Reddy G Madhusudhana, Sammaiah P, Murthy CVS, Mohandas T. Influence of welding techniques on microstructure and mechanical properties of AA 6061 (Al–Mg–Si) gas tungsten arc welds. in: Proceedings of national conference on processing of metals, Coimbatore. 2002. p. 33–46.
- [2] Kou S, Le Y. Nucleation mechanism and grain refining of weld metal. *Weld J* 1986;65–70.
- [3] Prasad Rao K, Reddy GM, Gokhale AA. Grain refinement and improvement of strength and ductility of welds by pulsed current and magnetic arc oscillation techniques. International welding conference, New Delhi. 1999. p. 1050–5.
- [4] Thomas WM, et al. Friction stir welding. International Patent Application No. PCT/GB92/02203 and GB Patent Application No. 9125978.8, December 1991, US Patent No. 5,460,317, 1991.
- [5] Threadgill PL. Friction stir welding – The state of the art, Bulletin 678, TWI, UK, 1999.
- [6] Peel M, Steuwer A, Preuss M, Withers PJ. Microstructure, mechanical properties and residual stresses as a function of welding speed in AA5083 friction stir welds. *Acta Mater* 2003;51:4791–801.
- [7] Murr LE, Flores RD, Flores OV, McClure JC, Liu G, Brown D. *Mate Res Innov* 1998;1:211.
- [8] Huijie Liu, Fujii H, Maeda M, Nogi K. Heterogeneity of mechanical properties of friction stir welded joints of 1050-H 24 aluminium alloy. *J Mater Sci Lett* 2003;22:441–4.
- [9] Liu HJ, Fujii H, Maeda M, Nogi K. Mechanical properties of friction stir welded joints of 1050-H 24 aluminium alloy. *Sci Technol Weld Join* 2003;8:450–4.
- [10] Thomas WM, Dolby RE. Friction stir welding developments. in: Proceedings of 6th international trends in welding research conference, 2002. p. 203–11.
- [11] Thomas WM, Nicholas ED. Friction stir welding for the transportation industries. *Mater Des* 1997;18:269–73.
- [12] Colligan K. Material flow behaviour during friction stir welding of aluminium. *Weld J* 1999;229s–37s.
- [13] Ouyang JH, Jandric D, Kovacevic R, Song M, Valant M. Visualization of material flow during friction stir welding (FSW) of the same and dissimilar aluminum alloys. in: Proceedings of 6th international trends in welding research, 2002. p. 229–40.
- [14] Ying Li, Murr LE, McClure JC. Solid state flow visualization in the Friction stir welding of 2024Al to 6061Al. *Scripta Mater* 1999;40(9):1041–6.
- [15] Lima EBF, Wegener J, Dalle Donne, Goerigk G, Wroblewski T, Buslaps T, et al. Dependence of the microstructure, residual stresses and texture of AA6013 friction stir welds on the welding processes. *Z Metallkd* 2003;94(8):908–15.
- [16] Oosterkamp A, Djapic Oosterkamp L, Nordeide A. Kissing bond phenomena in solid state welds of aluminum alloys. *Weld J* 2004;225s–31s.